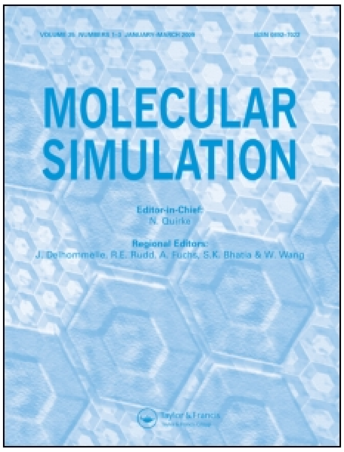

Molecular Simulation
Publication details, including instructions for authors and subscription information:
http://www.informaworld.com/smpp/title~content=t713644482

A Study of Thin Film $YBa_2Cu_3O_{6.5}$/MgO Interfaces Using a Near Coincidence Site Lattice Theory with Atomistic Simulation

D. C. Sayle[a]; S. C. Parker[a]; J. H. Harding[b]
[a] School of Chemistry, University of Bath, Avon, United Kingdom [b] AEA Technology, B424.4, Harwell Laboratory, Didcot, Oxfordshire, United Kingdom

To cite this Article Sayle, D. C. , Parker, S. C. and Harding, J. H.(1994) 'A Study of Thin Film $YBa_2Cu_3O_{6.5}$/MgO Interfaces Using a Near Coincidence Site Lattice Theory with Atomistic Simulation', Molecular Simulation, 12: 2, 127 — 139
To link to this Article: DOI: 10.1080/08927029408022529
URL: http://dx.doi.org/10.1080/08927029408022529

Molecular Simulation, 1994, Vol. 12, pp. 127–139
Reprints available directly from the publisher
Photocopying permitted by license only

A STUDY OF THIN FILM $YBa_2Cu_3O_{6.5}$/MgO INTERFACES USING A NEAR COINCIDENCE SITE LATTICE THEORY WITH ATOMISTIC SIMULATION

D.C. SAYLE, S.C. PARKER

School of Chemistry, University of Bath, Avon, United Kingdom BA1 7AY

J.H. HARDING

AEA Technology, B424.4, Harwell Laboratory, Didcot, Oxfordshire, United Kingdom OX11 DRA

(Received June 1993, accepted June 1993)

A near coincidence site lattice theory is employed in conjunction with atomistic simulation to elucidate the interfacial stability and detailed interfacial structural configurations for $YBa_2Cu_3O_{6.5}$ thin films on an MgO substrate observed experimentally. The interfacial stability is found to be dependent on the misfit.

KEY WORDS: Thin films, interfacial stability

1 INTRODUCTION

The formation of superconducting thin films is fundamental to their application in electronic devices [1, 2]. The effect of the substrate may modify or even have deleterious effects on the superconducting properties [3–11]. This may, in part, be addressed by computer simulation where one can obtain an insight into the detailed atomic structure, particularly the structure at the interface. In this paper we attempt to demonstrate the scope of atomistic simulation techniques, by calculating the effect of an interface on the structure of a ceramic oxide.

In this paper we investigate $YBa_2Cu_3O_{6.5}$(001) thin films on an MgO(100) substrate. We employ the simulation techniques to identify the stability of the various interfaces, the most stable $YBa_2Cu_3O_{6.5}$ plane with which to interface to the MgO, the factors responsible for influencing the stability and finally any structural modifications of the $YBa_2Cu_3O_{6.5}$ film as a result of the interface. We employ a Near Coincidence Site Lattice Theory (NCSL) to investigate the interfacial relationships observed experimentally [12] between the $YBa_2Cu_3O_{6.5}$/MgO interfaces. This theory was first employed in conjunction with atomistic simulation to investigate the BaO(100)/MgO(100) and CeO_2(111)/Al_2O_3(001) interfaces in an earlier paper [13].

2 METHODOLOGY

We generate an initial structure using a modified coincidence site lattice theory; the energies of the resulting configurations are obtained from a full energy minimisation.

2.1 *Near coincident site lattice theory (NCSL)*

Near coincidence site lattice theory is a special case of the coincidence site lattice theory [14] (CSL). For heteroepitaxial interfaces, the non-commensurate relationship between the lattice parameters of the two materials mean that an exact coincidence cannot be found and hence a lattice misfit or near coincidence is introduced. The theory will be outlined for simple cubic systems and then applied to construct $YBa_2Cu_3O_{6.5}$(001)/MgO(100) interfaces with low associated misfits.

The interphase boundaries of two materials with lattice parameters a_1 and a_2 can be considered as two-dimensional square lattices for cubic systems. A two-dimensional coincidence site lattice is produced by rotating one lattice with respect to the other about the axis normal to the interface (Figure 1) until three lattice sites of the two materials are in common. Exact coincidence occurs when

$$(\mathbf{a_1}/\mathbf{a_2})^2 = (\mathbf{m}^2 + \mathbf{n}^2)/(\mathbf{k}^2 + \mathbf{l}^2) \tag{1}$$

where **m,n,k** and **l** are integers. The rotational angle associated with this coincidence site lattice to bring the two crystals into exact coincidence is:

$$\Theta = \tan^{-1}(\mathbf{n}/\mathbf{m}) \pm \tan^{-1}(\mathbf{l}/\mathbf{k}) \tag{2}$$

The four fold symmetry of the square lattices ensure both positive and negative values of Θ give equivalent interfaces and therefore only values between 0 and 45° need to be considered.

The density of planar coincidence sites Γ is defined as $(1/\Sigma_1^p)$ where Σ_1^p is the planar reciprocal coincidence density at the interface and is given by:

$$\sum\nolimits_1^p = (\mathbf{m}^2 + \mathbf{n}^2) \tag{3}$$

$$\sum\nolimits_2^p = (\mathbf{k}^2 + \mathbf{l}^2) \tag{4}$$

The subscript p is used to denote a planar two dimensional coincidence [15]. Exact coincidence only occurs when equation (1) is satisfied exactly (i.e. $a_1 = a_2$). However, this relationship can never be satisfied exactly for heteroepitaxial systems. The incommensurate relationship between the lattice parameters (for all known lattice parameters) ensures that the left hand side of the equation (1) is irrational whilst the right hand side is always rational. Equation (1) can only be satisfied exactly if either one or both of the lattice parameters are changed i.e. if the crystals are expanded or contracted with respect to their optimum lattice parameter. This may be facilitated by matching the two materials at a particular temperature where the differences in the coefficients of linear expansion enable a particular NCSL to be in exact coincidence.

The misfit, F, which must therefore be accommodated by the expansion or

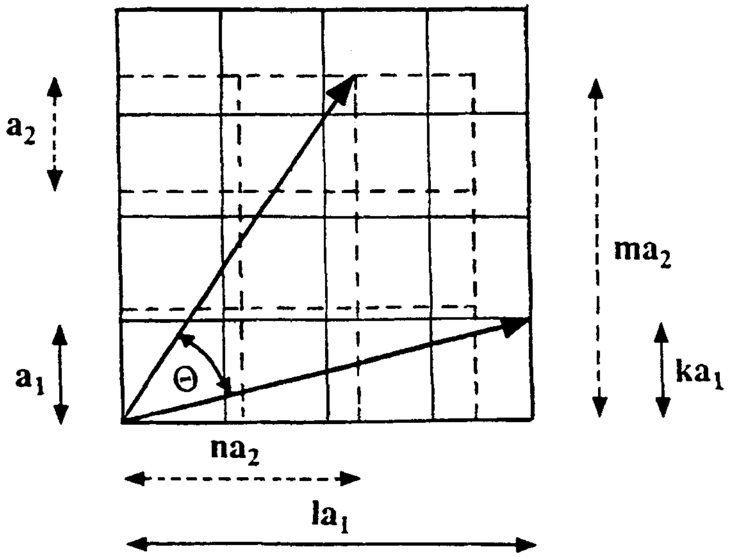

Figure 1 Schematic representation of the interphase boundaries between two materials of lattice parameters a_1 and a_2 for cubic systems; where k,l,m and n are integers and Θ is the rotational angle of one material with respect to the other.

contraction of the crystals is defined as the deviation from the exact coincidence condition, and designated a Near Coincidence Site Lattice (NCSL). This misfit is given by:

$$F = 2\left(\left|a_1\sqrt{\Sigma_1^p} - a_2\sqrt{\Sigma_2^p}\right|\right) \Big/ \left(a_1\sqrt{\Sigma_1^p} + a_2\sqrt{\Sigma_2^p}\right) \tag{5}$$

A low value for the misfit resulting in a small loss in strain energy can always be achieved by increasing the size of Σ^p. However, this increase may cause the size of the resulting primitive unit cell to become prohibitively large even for modern computers.

A further problem one must address is that $YBa_2Cu_3O_{6.5}$ is orthorhombic [16, 17]. Near coincidence site lattice theory can predict interface construction for orthorhombic systems grown on a cubic substrate [18, 19]. However, the size of the cell required to accommodate this interface is, as yet, too large to consider computationally. To accommodate the primitive unit cell within the computer resources we have available, the $YBa_2Cu_3O_{6.5}$ must be constrained to tetragonal, rather than orthorhombic symmetry. This will necessitate modifying the a_0 and b_0 lattice parameters of the $YBa_2Cu_3O_{6.5}$ structure. This change in lattice parameter is small compared to the adjustment of the $YBa_2Cu_3O_{6.5}$ required to accommodate the misfit. Extensive work by Kenway [20] shows that the material properties of tetragonal and orthorhombic symmetries are similar providing justification for this approach.

Table 1 Short range potential parameters for $MgO^{[24]}$ and $YBa_2Cu_3O_{6.5}^{[25]}$.

$YBa_2Cu_3O_{6.5}$ Interaction	$\Phi(r_{ij}) = A\exp[(-\lvert r_i - r_j\rvert)/p] - Cr^6$ A(eV)	p(Å)	C(eV/Å^6)
$Y^{3+} - Y^{3+}$	–	–	–
$Y^{3+} - Ba^{2+}$	–	–	–
$Y^{3+} - Cu^{2+}$	–	–	–
$Y^{3+} - O^{2-}$	20717.5	0.24203	0.0
$Ba^{2+} - Ba^{2+}$	2663.7	0.2588	0.0
$Ba^{2+} - Cu^{2+}$	168128.6	0.22873	0.0
$Ba^{2+} - O^{2-}$	3115.5	0.33583	0.0
$Cu^{2+} - Cu^{2+}$	–	–	–
$Cu^{2+} - O^{2+}$	3799.3	0.24273	0.0
$O^{2-} - O^{2-}$	22764.0	0.1490	75.0

b) Shell Parameters

Ion	Y	k(eV/Å^2)
Y^{3+}	Rigid Ion	
Ba^{2+}	9.1173	426.1
Cu^{2+}	Rigid Ion	
O^{2-}	−3.2576	49.8

c)

MgO Interaction	$\Phi(r_{ij}) = A\exp[(-\lvert r_i - r_j\rvert)/p] - Cr^{-6}$ A(eV)	p(Å)	C(eV/Å^6)
$Mg^{2+} - O^{2-}$	1428.5	0.2945	0.0
$O^{2-} - O^{2-}$	22764.3	0.149	27.879

d) Shell Parameters

Ion	Y	k(eV/Å^2)
Mg^{2+}	Rigid Ion	
O^{2-}	−3.0	51.836

Short Range cutoff = 15Å.

2.2 *Simulation code and potential model*

The simulations in this work were performed on the CRAY X-MP4/8 at the Atlas Division of Rutherford Appleton laboratory using the energy minimisation code MIDAS [21]. The interionic potentials are based on the Born model of ionic solids [22], which includes a long range coulombic interaction and a short range term to model the repulsions and Van der Waals attractions between electron charge clouds. The shell model [23] was used to describe the electronic polarisability of the component ions.

The interionic potentials used were derived by Lewis and Catlow [24] for MgO and for $YBa_2Cu_3O_{6.5}$ the potentials derived by Baetzold [25] were employed. The potentials are presented in table 1.

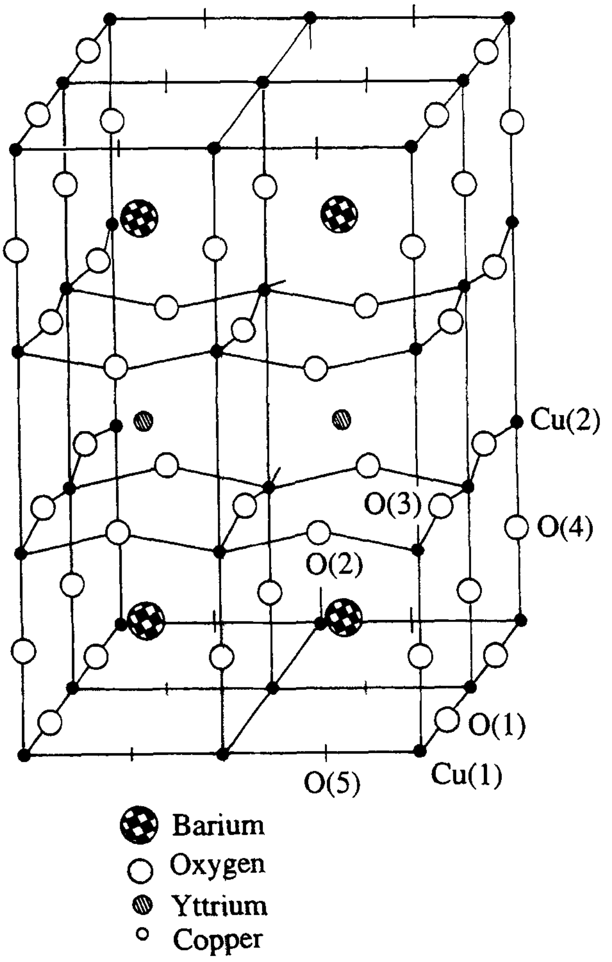

Figure 2 Diagrammatic representation of the orthorhombic II $YBa_2Cu_3O_{6.5}$ structure indicating ion site notation.

3 RESULTS

3.1 *$YBa_2Cu_3O_{6.5}$ structure*

The structure of $YBa_2Cu_3O_{6.5}$ is shown in figure 2. The oxygen O(1) ions in the CuO basal plane of the $YBa_2Cu_3O_{6.5}$ can be ordered by careful heat treatment resulting in a doubling of the a_0 and/or b_0 lattice parameters in one or two directions resulting in a more stable $YBa_2Cu_3O_{6.5}$ structure [26]. This orthorhombic II structure cannot be considered because the size of the primitive unit cell becomes prohibitively large. In this work we consider two alternative $YBa_2Cu_3O_{6.5}$ structures for the thin film. These are designated Type A and Type B (figures 3 and 4) respectively. Type A is constructed such that the oxygen O(1) positions from

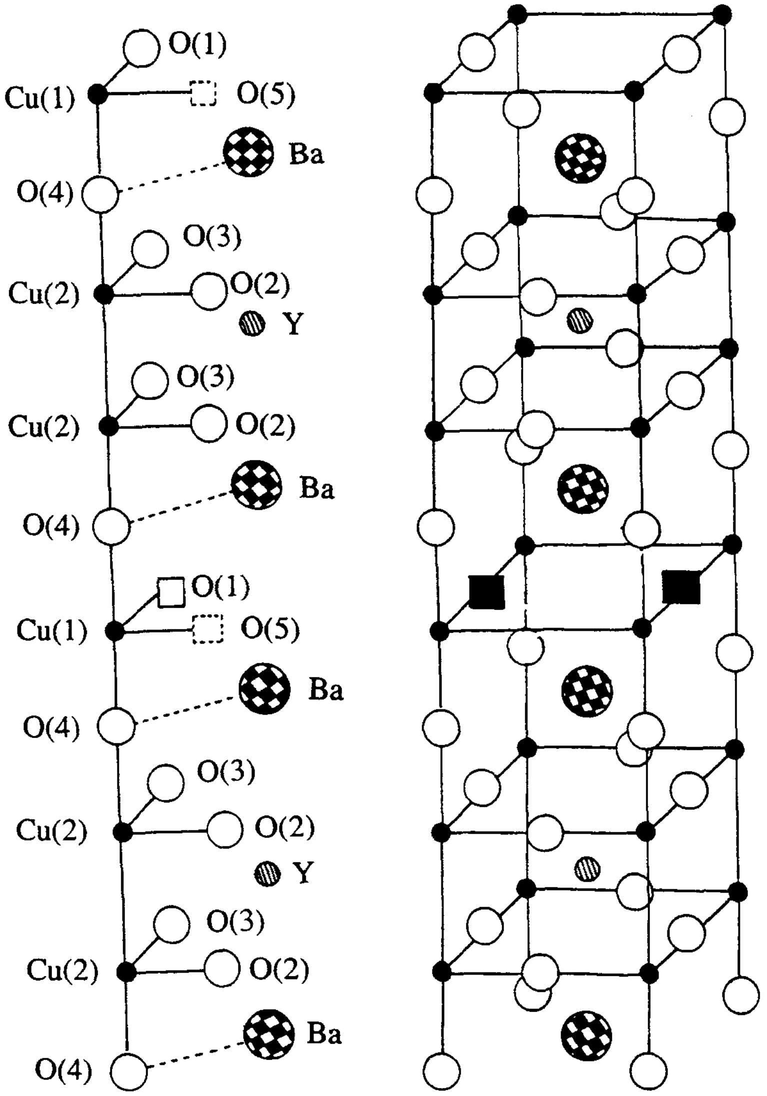

Figure 3 Diagrammatic representation of $YBa_2Cu_3O_{6.5}$ type A structure indicating ion site notation. To the left of the figure is the primitive unit cell. Note nonequivalent ions may be similarly labelled to ensure consistency with most experimental work which ascertains only the average structural configuration as opposed to local structural variation and therefore does not allow for the identification of these nonequivalent ions.

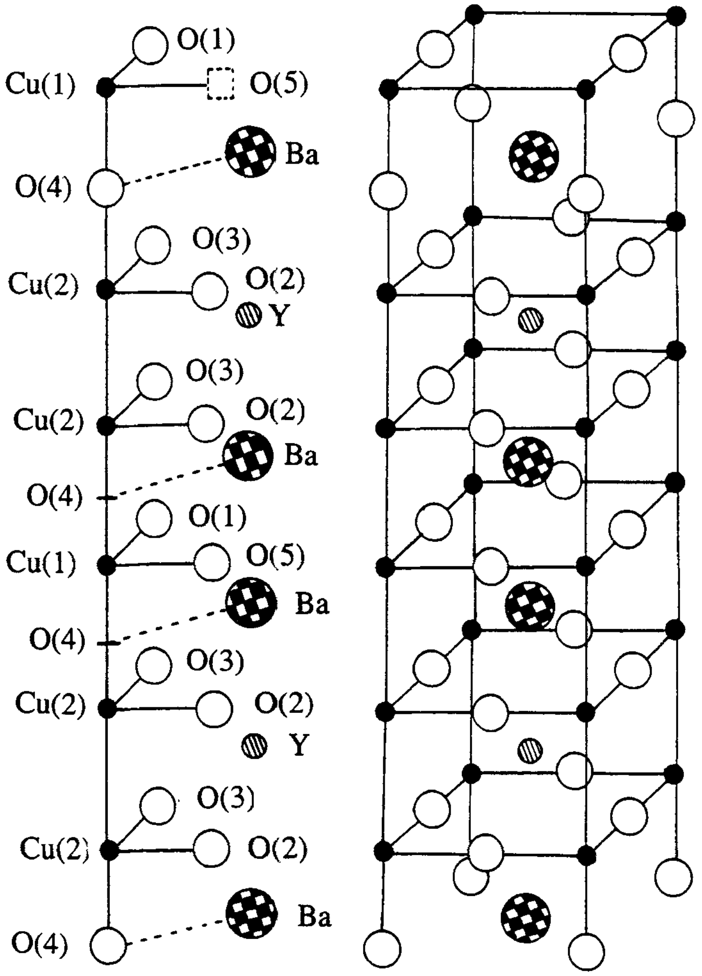

Figure 4 Diagrammatic representation of $YBa_2Cu_3O_{6.5}$ type B structure indicating ion site notation. To the left of the figure the primitive unit cell is shown.

alternate Cu(1)O(1) planes are empty as opposed to the observed 50% O(1) occupancy on every Cu(1)O(1) plane (figure 2). Type B differs from Type A structure by a substitution of the O(4) oxygens to fill the O(1) and O(5) positions.

The calculated energy of the unit cell of the $YBa_2Cu_3O_{6.5}$ Type A structure is −523.78 eV and Type B, −523.83 eV. This compares to −524.82 eV for the $YBa_2Cu_3O_{6.5}$ orthorhombic II structure. The 0.02% difference is sufficiently small to believe that these structures represent reasonable models of the fine structure. Furthermore, the structure of the $YBa_2Cu_3O_{6.5}$ was elucidated by neutron diffraction [16, 17], which determines the average structure and may therefore exhibit local structural deviations from the average orthorhombic II structure. Indeed, several workers have identified deviations from the average structural configurations [27-30].

Table 2 Near coincidence site lattices (NCSL) for the $YBa_2Cu_3O_{6.5}(001)//MgO(100)$ interfaces calculated for $YBa_2Cu_3O_{6.5}$ structural types A and B assuming lattice parameters of 3.875 Å and 3.915 Å respectively.

$\Sigma^p_{YBCO}\Sigma^p_{MgO}$	k	l	m	n	Θ	*Misfit/%* *Type A*	*Type B*
1/1 α	1	0	1	0	0	+8.05	+7.02
5/4 β	2	1	2	0	26.565	−3.10	−4.13
9/8 β	3	0	2	2	45	+2.16	+1.14
10/9 β	3	1	3	0	18.435	+2.79	+1.76
16/13 β	4	0	3	2	33.690	−2.33	−3.35
20/17 β	2	4	1	4	12.529,40.601*	−0.07	−1.10
25/20 β	3	4	2	4	10.305	−3.10	−4.13
29/25 α	2	5	3	4	15.068*,31.329	+0.63	+0.39
29/25 α	5	2	5	0	21.801	+0.63	+0.39

*Not Observed Experimentally.

3.2 *$YBa_2Cu_3O_{6.5}(001)/MgO(100)$ interfaces*

Table 2 shows the interfaces predicted for $YBa_2Cu_3O_{6.5}(001)/MgO(100)$ (Type A and Type B) using a near coincidence site lattice theory. All these interfaces have been observed experimentally and are therefore expected to be stable. The lattice parameters of the $YBa_2Cu_3O_{6.5}$ structures are calculated to be $a_0 = b_0 = 3.885$ Å (Type A) and $a_0 = b_0 = 3.915$ Å (Type B).

Three $YBa_2Cu_3O_{6.5}(001)/MgO(100)$ systems were investigated computationally:

1) $$\sum\nolimits^p_{YBCO}\sum\nolimits^p_{MgO} = \mathbf{1/1}(\Theta = 0°),$$

2) $$\sum\nolimits^p_{YBCO}\sum\nolimits^p_{MgO} = \mathbf{5/4}(\Theta = 26.565°),$$

3) $$\sum\nolimits^p_{YBCO}\sum\nolimits^p_{MgO} = \mathbf{20/17}(\Theta = 12.529°)$$

The MgO substrate is constrained to its natural lattice parameter and the $YBa_2Cu_3O_{6.5}$ is therefore required to accommodate the full misfit. The interfaces were considered with one $YBa_2Cu_3O_{6.5}$ unit cell on the MgO(100) surface. We first consider the $\Sigma^p_{YBCO}\,\Sigma^p_{MgO} = \mathbf{1/1}(\Theta = 0°)$ interface. This interface can be constructed with the $YBa_2Cu_3O_{6.5}(001)$ plane terminating with either CuO, CuO_2, Y, BaO, or Cu at the $YBa_2Cu_3O_{6.5}/MgO$ interface. Construction of the system with Y, Cu or CuO_2 at the interface results in a dipole moment in the $YBa_2Cu_3O_{6.5}$ normal to the interface. This causes a divergence of the electrostatic energy [31]. Therefore only interfaces with BaO or CuO at the interface were considered.

Table 3 shows the interfacial energies, in Jm^{-2}, of the $YBa_2Cu_3O_{6.5}(001)/MgO(100)$, $\Sigma^p_{YBCO}\,\Sigma^p_{MgO} = \mathbf{1/1}(\Theta = 0°)$, type A and B interfaces with CuO and BaO planes terminating the $YBa_2Cu_3O_{6.5}$ at the interface. The interfacial energies represent the energy required to cleave the interface to form a pure MgO surface and an $YBa_2Cu_3O_{6.5}$ monolayer thin film per unit interfacial area.

$$\Delta\mathbf{E} = [(\mathbf{E}_{Overlayer} + \mathbf{E}_{Substrate}) - \mathbf{E}_{Interface}]/\mathbf{Area} \qquad (6)$$

Table 3 Calculated interfacial energies of the $YBa_2Cu_3O_{6.5}(001)//MgO(100)$, $\Sigma^P = 1/1$ ($\Theta = 0^\circ$) interfaces for $YBa_2Cu_3O_{6.5}$ structural types A and B with CuO and BaO planes terminating the $YBa_2Cu_3O_{6.5}$ at the interface region.

$YBa_2Cu_3O_{6.5}$ Structural Type	*Interfacial Stability/Jm^{-2} Initial*	*Final*	*Interfacial $YBa_2Cu_3O_{6.5}$ Plane*
Type A	−4.00	−2.21	BaO
Type A	−2.73	−0.71	CuO
Type B	−3.59	−2.02	BaO
Type B	−2.28	−0.51	CuO

Table 4 Calculated $YBa_2Cu_3O_{6.5}$ structural type A bond lengths in the $YBa_2Cu_3O_{6.5}(001)//MgO(100)$, $\Sigma^P = 1/1$ ($\Theta = 0^\circ$) interface with CuO plane terminating the $YBa_2Cu_3O_{6.5}$ at the interface region. The calculated bond lengths for pure $YBa_2Cu_3O_{6.5}$ type A are also given as a comparison. Bond lengths are in Angstroms.

Bond	*Pure $YBa_2Cu_3O_{6.5}$*		*Interfaced $YBa_2Cu_3O_{6.5}$*		*Difference*	
Ba-O(4)	2.74	2.97	2.93	3.27	0.19	0.30
Ba-O(2)	3.09	2.84	3.17	2.91	0.08	0.07
Ba-O(3)	3.10	2.84	3.18	2.87	0.08	0.03
Ba-O(1)	2.85		2.90		0.05	
Y-O(2)	2.31	2.49	2.38	2.60	0.07	0.11
Y-O(3)	2.31	2.50	2.37	2.59	0.06	0.09
Cu(1)-O(4)	1.99	1.80	1.83	1.80	−0.16	0.00
		1.80		1.80		0.00
Cu(1)-O(1)	1.94		2.08		0.14	
Cu(2)-O(4)	3.43	1.96	3.16	1.86	−0.27	−0.10
Cu(2)-O(2)	2.02	1.95	2.13	2.07	0.11	0.12
Cu(2)-O(3)	2.02	1.95	2.14	2.01	0.12	0.06

The calculaled stabilities for these interfaces (table 3) are all negative indicating that the interface is unstable with respect to an MgO(100) surface and an $YBa_2Cu_3O_{6.5}$ thin film. This is not an unreasonable result as the misfit is very high (8.05% and 7.02% for Type A and Type B respectively). This is in contrast to experimental work [12, 32]. A recent paper by Sayle *et al.*, however, suggests that interfaces with high misfits are unstable [13]. We tentatively suggest that the experimentally observed interface; $\Sigma^{p}_{\mathrm{YBCO}}\ \Sigma^{p}_{\mathrm{MgO}} = \mathbf{1/1}(\Theta = 0^\circ)$, has been incorrectly assigned.

Figure 5 shows diagrammatically the relaxed structure of the $\Sigma^{p}_{YBCO}\ \Sigma^{p}_{MgO} = \mathbf{1/1}(\Theta = 0^\circ)$ ($YBa_2Cu_3O_{6.5}$ Type A) interface with the $YBa_2Cu_3O_{6.5}$ CuO plane terminating at the interface region. In this figure the MgO oxygens at the interface region directly below the copper ions from the $YBa_2Cu_3O_{6.5}$ are displaced 0.48 Å towards the copper ions and the magnesium ions directly below the $YBa_2Cu_3O_{6.5}$ oxygens are displaced 0.29 Å towards the oxygens enhancing the favourable cation-anion interactions across the interface. The modification of the $YBa_2Cu_3O_{6.5}$ structure as a result of interfacing with the MgO substrate is of paramount importance to the superconducting properties of the material. Indeed, small changes in bond lengths greatly affect the superconducting transition temperature (T_c) of the material [33, 34, 35].

The structural modifications of the $YBa_2Cu_3O_{6.5}$ as a result of the relaxation are not apparent from inspection of the structure and therefore the relaxation of the

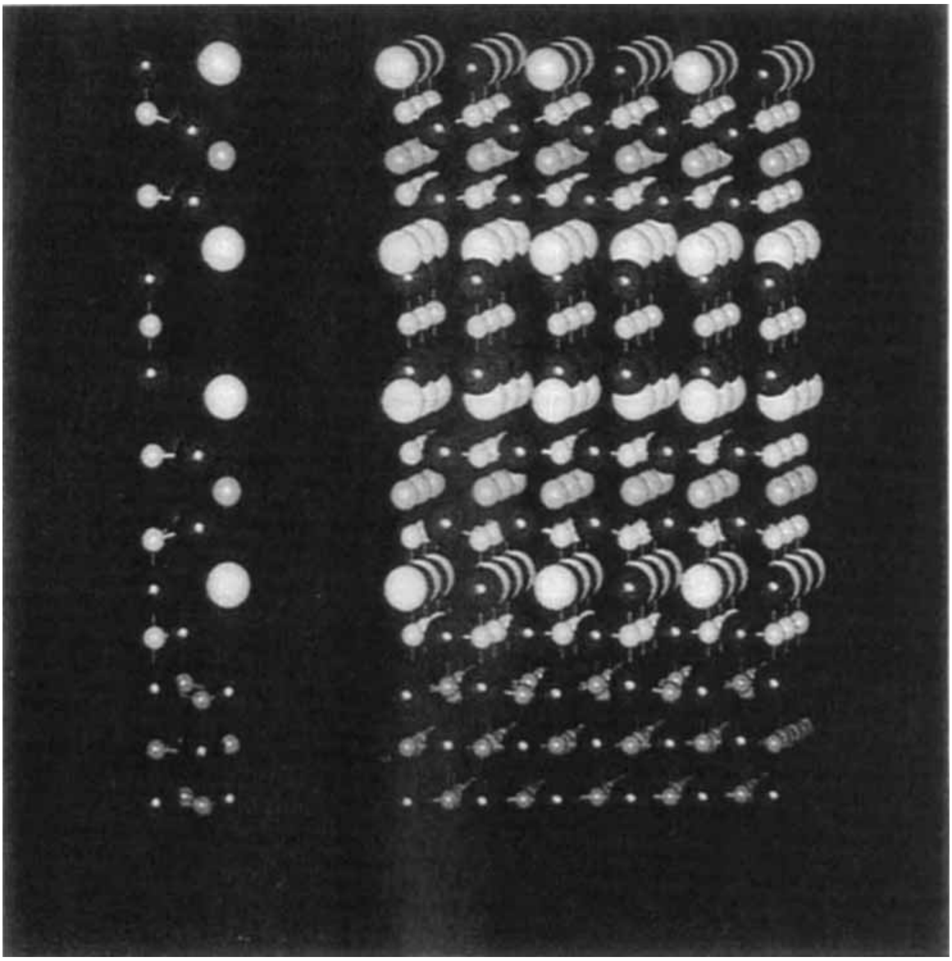

Figure 5 Calculated relaxed $YBa_2Cu_3O_{6.5}(001)//MgO(100)$, $\Sigma^P = 1/1$ ($\Theta = 0°$) type A interface structure. A CuO plane terminates the $YBa_2Cu_3O_{6.5}$ at the interface region. Oxygen is coloured red, barium is white, yttrium is yellow, copper is blue and magnesium is purple (see colour plates).

Table 5 Calculated interfacial energies of the $YBa_2Cu_3O_{6.5}(001)//MgO(100)$, $\Sigma^P = 5/4$ ($\Theta = 26.565°$) interfaces for $YBa_2Cu_3O_{6.5}$ structural types A and B with CuO and BaO planes terminating the $YBa_2Cu_3O_{6.5}$ at the interface region.

$YBa_2Cu_3O_{6.5}$ Structural Type	*Interfacial Stability/Jm^{-2} Initial*	*Final*	*Interfacial $YBa_2Cu_3O_{6.5}$ Plane*
Type A	−2.31	−0.82	BaO
Type A	−2.31	+0.16	CuO
Type B	−2.95	−1.29	BaO
Type B	−2.88	−0.14	CuO

$YBa_2Cu_3O_{6.5}$ is monitored by inspection of the bond lengths. Table 4 shows the calculated $YBa_2Cu_3O_{6.5}$ (Type A) bond lengths for the pure structure, compared to bond lengths calculated for the structure when interfaced to MgO. The $YBa_2Cu_3O_{6.5}$ bond lengths are observed to change by as much as 10% as a result of the interface.

The second system studied is the $\Sigma^{\rho}_{\mathrm{YBCO}}\ \Sigma^{\rho}_{\mathrm{MgO}} = \mathbf{5/4}(\Theta = 26.565^\circ)$ Two interfaces were considered for both structural types A and B, first with the CuO plane terminating the $YBa_2Cu_3O_{6.5}$ at the interface and second with the BaO plane terminating the $YBa_2Cu_3O_{6.5}$ at the interface. Table 5 gives the energies of the relaxed interfaces relative to the relaxed surface energy of the MgO surface and the $YBa_2Cu_3O_{6.5}$ thin film. An energy of $+0.16\ \mathrm{Jm}^{-2}$ is calculated for the $\Sigma^{\rho}_{\mathrm{YBCO}}\ \Sigma^{\rho}_{\mathrm{MgO}} = \mathbf{5/4}(\Theta = 26.565^\circ)$ CuO (Type A) suggesting that the interface is stable with respect to a pure MgO surface and $YBa_2Cu_3O_{6.5}$ thin film. The interfaces with the CuO planes terminating the $YBa_2Cu_3O_{6.5}$ are calculated to be more stable than with BaO terminating the $YBa_2Cu_3O_{6.5}$ at the interface.

The $YBa_2Cu_3O_{6.5}$(001)/MgO(100) interfaces investigated thus far have required the $YBa_2Cu_3O_{6.5}$ thin film to be expanded by 8.05 and 7.02% for the $\Sigma^{\rho} = 1/1$ configuration for $YBa_2Cu_3O_{6.5}$ structural types A and B respectively, and compressed by 3.10 and 4.13% for the $\Sigma^{\rho} = 5/4$ configuration. From the work by Sayle *et al.* these high values of the misfit are expected to severely destabilise the interface [13] compared to an interface of much lower misfit.

The next interface considered is the $\Sigma^{\rho}_{\mathrm{YBCO}}\ \Sigma^{\rho}_{\mathrm{MgO}} = \mathbf{20/17}(\Theta = 12.529^\circ)$ CuO (Type A) which has a very low associated misfit of −0.07% ($YBa_2Cu_3O_{6.5}$ must be compressed to accommodate the misfit). Only one calculation on this interface has been performed because of the enormous size of the primitive unit cell resulting from this configuration. Following the results of Sayle *et al.* [13] the lower angle associated with the near coincidence site lattice was chosen on the basis that lower angle near coincidence site lattices are more stable. Indeed the higher angle $\Sigma^{\rho}_{\mathrm{YBCO}}\ \Sigma^{\rho}_{\mathrm{MgO}} = \mathbf{20/17}(\Theta = 40.601^\circ)$ system has not yet been observed experimentally [12, 32]. The CuO plane was chosen to terminate the $YBa_2Cu_3O_{6.5}$ at the interface as the results of the $\Sigma^{\rho}_{\mathrm{YBCO}}\ \Sigma^{\rho}_{\mathrm{MgO}} = \mathbf{5/4}(\Theta = 26.565^\circ)$ interfaces suggest termination with this plane to be more stable than terminating the $YBa_2Cu_3O_{6.5}$ with the BaO plane at the interface. Finally the MgO and $YBa_2Cu_3O_{6.5}$ structures were considered employing the rigid ion model to reduce further the resulting primitive cell size and therefore enabling the system to be adequately accommodated by the computer resources available.

The calculated unrelaxed and relaxed interfacial energies of the $\Sigma^{\rho}_{\mathrm{YBCO}}\ \Sigma^{\rho}_{\mathrm{MgO}} = \mathbf{20/17}(\Theta = 12.529^\circ)$ CuO (Type A) interface are $-0.40\ \mathrm{Jm}^{-2}$ and $+0.55\ \mathrm{Jm}^{-2}$ respectively. This is $0.39\ \mathrm{Jm}^{-2}$ more stable than the $\Sigma^{\rho}_{\mathrm{YBCO}}\ \Sigma^{\rho}_{\mathrm{MgO}} = \mathbf{5/4}$ $(\Theta = 26.565^\circ)$ CuO (Type A) interface. Furthermore the stability is expected to be increased with the inclusion of ionic polarisability into the calculation. In accordance with previous calculations [13], the calculated energies of the $YBa_2Cu_3O_{6.5}$(001)/MgO(100) interfaces are more stable for low associated misfits.

4 CONCLUSIONS

The major objective of this paper has been to ascertain the factors conducive to interfacial stability and to develop a method which will enable a complex interface to be constructed and examined theoretically. The $YBa_2Cu_3O_{6.5}$/MgO system was chosen to be a model system representative of a complex heteroepitaxial ceramic interface in an attempt to elucidate factors, conducive to the interfacial stability, which may not have been identified by examining more simple systems considered in a previous paper [13].

The near coincidence site lattice theory was employed to investigate the $YBa_2Cu_3O_{6.5}$(001)/MgO(100) interfaces and has enabled the interfacial stability of the various interfaces, observed experimentally [12, 32], to be calculated. Furthermore the calculations have shown the $YBa_2Cu_3O_{6.5}$(001)/MgO(100) interface to exhibit maximum stability if the $YBa_2Cu_3O_{6.5}$ is terminated with the CuO plane at the interface rather than termination with a BaO plane. This is in accordance with recent theoretical work on BaO/MgO interfaces which shows them to be relatively unstable [13, 36]. The $YBa_2Cu_3O_{6.5}$(001)/MgO(100) interfacial stabilities are calculated to increase with decreasing misfit in accordance previous work [13]. The $\Sigma^{\rho}_{YBCO}\ \Sigma^{\rho}_{MgO} = 20/17(\Theta = 12.529°)$, with the lowest associated misfit of -0.07%, exhibiting the highest interfacial stability of $+0.55\ Jm^{-2}$.

The ionic relaxation of the $YBa_2Cu_3O_{6.5}$ for the $YBa_2Cu_3O_{6.5}$(001)/MgO(100) interfaces shows deviations from the perfect $YBa_2Cu_3O_{6.5}$ crystal structure with bond length modifications of up to 10%. This has serious implications for the superconducting properties of the material including T_c [33–35].

Acknowledgements

We acknowledge financial and computational support from the SERC and to Biosym Inc. for use of their molecular graphics software.

References

[1] R. Simon, "High-T_c thin films and electronic devices", *Physics Today*, **44**, 64 (1991).

[2] D. Larbalestier, "Critical currents and magnetic applications of high-T_c Superconductors", *Physics Today*, **44**, 74 (1991).

[3] N.L. Allan and W.C. Mackrodt, "Calculated lattice and dynamic properties of ternary and quaternary cuprates related to high-T_c superconductivity", *J. Chem. Soc., Faraday Trans.* 2 **85**(5) 385 (1989).

[4] E. Olsson, A. Gupta, M.D. Thouless, A. Segmüller and D.R. Clarke, "Crack formation in epitaxial [110] thin films of $YBa_2Cu_3O_{7-\delta}$ and $PrBa_2Cu_3O_{7-\delta}$ on [110] $SrTiO_3$ substrates" *Appl. Phys. Lett.*, **58** 1682 (1991).

[5] S.A. Kramer, G. Kordas, J. McMillan, G.C. Hilton and D.J. Van Harligen, "Highly oriented superconducting thin films derived from the sol-gel process", *Appl. Phys. Lett.*, **53**, 156 (1988).

[6] O.M. Bakunin, S.M. Klotsman, S.A. Matveev and K.A. Stepanov, "Oscillations of composition near the external surface of Y-Ba-Cu-O thin films", *Appl. Phys. Lett.*, **55**, 78 (1989).

[7] F.K. LeGoues, "The microstructure of $YBa_2Cu_3O_{7-x}$ thin films on $SrTiO_3$ substrate", *Phil. Mag. B.*, 57, 167 (1988).

[8] J. Kwo, T.C. Hseih, R.M. Fleming, M. Hong, S.H. Liou, B.A. Davidson and L.C. Feldman, "Structural and superconducting properties of orientation-ordered $YBa_2Cu_3O_{7-x}$ films prepared by molecular-beam epitaxy", *Phys. Rev. B*, **36**, 4039 (1987).

[9] C.H. Chen, J. Kwo and M. Hong, "Microstructures of $YBa_2Cu_3O_{7-x}$ superconducting thin films grown on a $SrTiO_3$(100) substrate", *Appl. Phys. Lett.*, **52**, 841 (1988).

[10] O. Eibl, H.E. Hoenig, J.-M. Triscone, O. Fischer, L. Antognazza and O. Brunner, "Micro-

structure of $YBa_2Cu_3O_7/PrBa_2Cu_3O_7$ superlattices deposited on (100) $SrTiO_3$ single crystals", *Physica C*, **172**, 365 (1990).

[11] J. Narayan, S. Sharan, R.K. Singh, K. Jagannadham, "Misfit dislocations in superconducting thin-films on $SrTiO_3(010)$", *Mater. Sci. Eng.*, **B2**, 333 (1989).

[12] D.M. Hwang, T.S. Ravi, R. Ramesh, Siu-Wai Chan, C.Y. Chen, L. Nazar, X.D. Wu, A. Inam, T. Venkatesan, "Application of a near coincidence site lattice theory to the orientations of $YBa_2Cu_3O_{7-x}$ grains on (001) MgO substrates", *Appl. Phys. Lett.*, **57**, 1690 (1990).

[13] T.X.T. Sayle, C.R.A. Catlow, D.C. Sayle, S.C. Parker and J.H. Harding, "Computer simulation of heteroepitaxial ceramic interfaces using a near coincidence site lattice theory" *Phil. Mag*-in press.

[14] H. Grimmer, W. Bollmann, D.H. Warrington, "Coincidence-site lattices and complete pattern shift lattices in cubic materials", *Acta. Cryst.*, **30**, 197 (1974).

[15] Y. Gao, P. Shewmon, S.A. Dreigia, "Coincidence interphase boundaries in MgO/Ni system", *Scripta Metallurgica*, **22**, 1521 (1988).

[16] S. Miraglia, F. Beech, A. Santoro and D. Tran Qui, "Neutron Powder Diffraction Study of Orthorhombic $YBa_2Cu_3O_{6.5}$", *Mat. Res. Bull. Vol. 22*, 1733 (1987).

[17] J.D. Jorgensen, B.W. Veal, A.P. Paulikas, L.J. Nowicki, G.W. Crabtree, H. Claus and W.K. Kwok, "Structural properties of oxygen deficient $YBa_2Cu_3O_{7-\delta}$" *Phys. Rev. B*, **41**, 1863 (1990).

[18] R. Kern, "Crystal growth in science and technology", Ed. H. Arend, J. Hullinger (NATO ASI series, NY plenum) pp 143–169 (1989).

[19] A. Lamagna, S. Nicoletti, M. Sanchez Balmaseda, A. Migliori, R. Fabbri, L. Correra, "In-plane texture and transport properties of YBCO films grown on MgO cut off-axis", *Supercond. Sci. Technol.*, **5**, 117 (1992).

[20] P.R. Kenway, "Computer simulation of the pure and defective surface properties of α-aluminium oxide, lanthanum cuprate and neodymium cuprate", PhD thesis, University of Bath, 1991.

[21] P.W. Tasker, Harwell Report, "A guide to MIDAS a program for studying surfaces and interfaces in ionic crystals", AERE-R9130 (1978).

[22] M. Born, K. Hwang, "Dynamical theory of crystal lattices" (Oxford university press 1954).

[23] B.G. Dick and A.W. Overhauser, "Theory of the dielectric constants of alkali halide crystals", *Phys. Rev.*, **112**, 90 (1958).

[24] G.V. Lewis, C.R.A. Catlow, "Potential models for ionic oxides", *J. Phys. C*, **18**, 1149 (1985).

[25] R.C. Baetzold, "Atomistic simulation of ionic and electronic defects in $YBa_2Cu_3O_7$", *Phys. Rev. B*, **38**, 11,304 (1988).

[26] J. Kondo, "Oxygen ordering in YBCO", *J. Phys. Soc. Jpn.*, **59**, L819 (1990).

[27] H.W. Zandbergen, G. Van Tendeloo, T. Okabe and S. Amelinkx, "Electron diffraction and electron microscopy of the superconducting compound $Ba_2YCu_3O_{7-\delta}$", *Phys. Stat. Sol.*, **103**, 45 (1987).

[28] P. Fischer, J. Karpinski, E. Kaidis, E. Jilek and S. Rusieki, "High pressure preparation and neutron-diffraction study of the high-T_c superconductor $YBa_2Cu_4O_{8\pm x}$", *Sol. St. Comm.*, **69**, 531 (1989).

[29] A.W. Hewat, P. Fischer, E. Kaldis, J. Karpinski, S. Rusiecki, E. Jilek, "High-resolution neutron powder diffraction investigation of temperature and pressure effects on the high-T_c superconductor $Y_2Ba_4Cu_7O_{15}$", *Physica C*, **167**, 579 (1990).

[30] S. Amelinckx, G. Van Tendeloo and J. Van Landuyt, "The study of high-T_c-superconducting materials by electron microscopy and electron diffraction", *Supercond. Sci. Technol.*, **4**, S19 (1991).

[31] P.W. Tasker, "The stability of ionic crystal surfaces", *J. Phys. C: Solid State Phys.*, **12**, 4977 (1979).

[32] T.S. Ravi, D.M. Hwang, R. Ramesh, S.W. Chan, L. Nanar, C.Y. Chen, A. Inman, T. Venkatesan, "Grain boundaries and interfaces in Y-Ba-Cu-O films laser deposited on single-crystal MgO", *Phys. Rev. B*, **42**, 10,141 (1990).

[33] P.F. Miceli, J.M. Tarascon, L.H. Greene, P. Barboux, F.J. Rotella, J.D. Jorgensen, "Role of bond lengths in the 90 K superconductor- A neutron powder diffraction study of YBa_2Cu_3-$XCOXO_7$-Y", *Phys. Rev. B*, **37**, 5932 (1988).

[34] M.S. Islam and R.C. Baetzold, "Atomistic simulation of dopant substitution in $YBa_2Cu_3O_7$", *Phys. Rev. B*, **40**, 10,926 (1989).

[35] X. Zhang and C.R.A. Catlow, "Computer simulation study of pressure-induced structural changes in $YBa_2Cu_3O_8$", *Physica C*, **193**, 221 (1992).

[36] D.C. Sayle "Computer Simulation of heteroepitaxial oxide/oxide and metal/oxide interfaces", PhD thesis, University of Bath (1992).